Broadening and Shift Coefficients of H$_2$O Absorption Lines in the 8650−9020 cm^{-1} Spectral Region

V. M. Deichuli[a, b]**, T. M. Petrova**[a, *]**, Yu. N. Ponomarev**[a]**, A. M. Solodov**[a]**, and A. A. Solodov**[a, **]

[a]*V.E. Zuev Institute of Atmospheric Optics, Siberian Branch, Russian Academy of Sciences, Tomsk, 634055 Russia*
[b]*Tomsk State University, Tomsk, 634050 Russia*
*e-mail: tanja@iao.ru
**e-mail: asolodov@iao.ru

Abstract—The broadening and shift coefficients of H$_2$O absorption lines are compared for Ar, He, H$_2$, and N$_2$ buffer gases. The broadening and shift coefficients were derived from the analysis of the absorption spectra recorded with an FTIR spectrometer in the spectral region 8650−9020 cm^{-1} with a spectral resolution of 0.01 cm^{-1}. Using two model line profiles (Voigt and speed-dependent Voigt profiles) the parameters of the H$_2$O absorption lines were calculated. It is shown that the speed-dependent Voigt profile provides better agreement with experimental data.

The study of the absorption spectra of a water molecule is of unfailing interest due to its particular role in the Earth's atmosphere. Exact values of the broadening and shift coefficients of this molecule are required to be known for numerous applications.

Extraction of accurate and reliable information about the parameters of spectral lines of gases has been the focus of attention in recent years. It has been shown that the description of real absorption line profiles provided by the commonly used Voigt profile is insufficiently accurate [1−4], which results in errors when determining such line parameters as intensity and broadening coefficient. These errors can attain several percent even for isolated lines; they are maximal near the center and in the wings of spectral lines. This inaccuracy of the model can introduce a significant error in the concentration of a gas under study.

There are many models of the absorption line profiles, which take into account fine effects shown in the spectra of molecules. Quite simple profiles with a small number of physically clear approximation parameters are required for use in mass spectroscopic measurements in wide wavelength ranges. The purpose of this work is to compare the parameters of H$_2$O absorption lines derived with the use of different profiles from data sets for H$_2$O−Ar, H$_2$O−He, H$_2$O−H$_2$, and H$_2$O−N$_2$.

EXPERIMENTAL

The broadening and shift coefficients of the absorption lines of the H$_2$O molecule in the region 8650−9020 cm^{-1} were analyzed in our works [5−8] using the traditional Voight profile for H$_2$O−N$_2$ and H$_2$O−He and the Voight profile depended on the speed of active molecules for H$_2$O−H$_2$ and H$_2$O−Ar. All spectra were measured using a Bruker IFS 125HR Fourier transform spectrometer equipped with a tungsten light source and an InSb detector. This spectrometer has an evacuated sample compartment pumped out to a residual pressure of ~0.02 mbar with a fore pump, which significantly weakens the effect of atmospheric gases on the measurement results. The water pressure did not exceed 18 mbar, and the buffer gas pressure varied from 0 to 3100 mbar. Depending on the pressure of an H$_2$O−buffer gas mixture, three sensors were used: Baratron (measurement error 0.25%) in the pressure range 0−100 mbar, DVR5 (measurement accuracy 0.5%) in the range 100−1000 mbar, and DM501E (measurement accuracy 0.5%) in the range of 1000−3000 mbar. All absorption spectra were recorded at room temperature (296 K) with a spectral resolution of 0.01 cm^{-1} along a 10 m optical path in a cell. Table 1 presents the measurement conditions during the experiment.

The experimental setup and experimental technique are described in detail in [5−8].

RESULTS AND DISCUSSION

We considered 35 water absorption lines, either isolated or those for which it is easy to take into

Table 1. Pressure of a H_2O−buffer gas mixture, mbar

H_2O−Ar		H_2O−H_2		H_2O−N_2		H_2O−He	
17	282	16	684	17	288	10	261
18	593	16	488	15	588	10	602
18	890	8	417	17	905	10	1028
		10	415	6	298	10	2021
		17	334	6	619	10	2510
		18	181	6	971	10	3127

account closely spaced lines with lower intensity, with the Doppler half-width varying from 0.0125 to 0.0130 cm^{-1}. The signal-to-noise ratio was quite high, 1000 and more. In the spectral region 8650–9020 cm^{-1}, H_2O absorption lines were observed which belong to the vibrational bands $\nu_1 + \nu_2 + \nu_3$, $2\nu_1 + \nu_2$, $6\nu_2$, and $\nu_2 + 2\nu_3$. The strongest is the $\nu_1 + \nu_2 + \nu_3$ band. The broadening and shift coefficients were determined for this band.

To calculate the parameters, the software [9, 10] was used. It allows determining line parameters from their simultaneous fitting to several spectra recorded under different conditions. To approximate the experimental data, two profile models were used: the traditional Voigt profile (V) with a fixed Doppler half-width and the active molecule speed-dependent Voigt profile—quadratic speed-dependent Voigt (qSDV).

Narrowing of the spectral lines is cause by the so-called wind effect, which is due to the dependence of the collisional relaxation constants on the speed of active molecules. In this case, the Lorentz half-width and the line center shift are not constant and depend on the speed of the absorbing molecule.

To determine the line parameters using a qSDV profile, the fast calculation algorithm suggested in [11] was applied. The wind effect was also taken into account in the IUPAC (International Union of Pure and Applied Chemistry) recommended profile for isolated absorption lines [4]. The spectral line parameters, such as the line center position, intensity, broadening, shift, and narrowing coefficients were calculated for four data sets: H_2O–Ar, H_2O–He, H_2O–H_2, and H_2O–N_2.

Figure 1 shows the absorption line of the H_2O molecule centered at 8848.06925 cm^{-1}, broadened by the pressure of hydrogen, helium, nitrogen, and argon, as well as the difference between the experimental and calculated profiles. It should be noted that all these calculations were made with a fixed Doppler width. Each spectrum had its own base line, which was calculated using a first-order polynomial. Figure 1 shows that V cannot correctly describe a line observed, and the line narrowing effects should be taken into account, i.e., the narrowing due to the Dicke effect and the narrowing due to the wind effect. Since all the

spectra were recorded at a buffer gas pressures of more than 300 mbar, the wind effect makes the greatest contribution to the narrowing of the lines. The spectrum calculated with the help of the qSDV profile (see Fig. 1) coincides with the experimental spectrum. The standard deviation for the Voigt profile varied from 9×10^{-5} to 1.46×10^{-4}, while for qSDV profile it was lower and amounted to 5×10^{-5} to 8×10^{-5}.

The found parameters of H_2O spectral line broadening by different gases and corresponding confidence intervals are given in Tables 2 and 3.

Figures 2 and 3 show the H_2O broadening coefficients found with the two profiles. The lines in the tables and figures are grouped so as subbands in the rovibrational band $\nu_1 + \nu_2 + \nu_3$ manifest themselves.

Figure 3 shows in detail the dependences of the broadening coefficients of H_2O absorption lines on the rotational quantum number J for different buffer gases. Subbranches are shown for which the rotational quantum number K_a does not change, $K_a = 0$ (Fig. 3a) or 1 (Fig. 3b) for the upper and lower rovibrational states.

The water molecule interacts with the buffer gases considered in the work in different ways, since helium and argon are inert gases, while hydrogen and nitrogen are diatomic molecules. In addition, the masses of the molecules of these gases are significantly different. Therefore, the comparison of the parameters of H_2O absorption line broadening should be carried out for two groups.

(1) H_2O—an inert gas. In such systems, the electrostatic part of the interaction potential is zero, and the short-range part is the most important. Since the argon molecule is heavier than the helium molecule, the wind effect of the H_2O–Ar mixture is stronger; therefore, the narrowing coefficients are greater (see Table 2). The coefficients of H_2O broadening by helium and argon pressure are shown in Fig. 4a. The difference between the broadening coefficients obtained via approximation to qSDV and V profiles is small on the average and amounts to 0.00084 and 0.0018 cm^{-1} for helium and argon, respectively.

(2) H_2O—nonpolar diatomic molecules. The water molecule has a large dipole moment, and the N_2 and H_2 molecules are nonpolar, their dipole moments are zero; therefore, during collisions, the main interactions are dipole−quadrupole. The N_2 molecule has a larger quadrupole moment than H_2, which explains the large broadening coefficients. Since the nitrogen molecule is heavier than the hydrogen molecule, narrowing coefficients are high for a H_2O–N_2 mixture due to the dependence on the active molecule speed. The difference between the broadening coefficients obtained via approximation to qSDV and V profiles is 0.0017 and 0.0035 cm^{-1} on average for hydrogen and nitrogen.
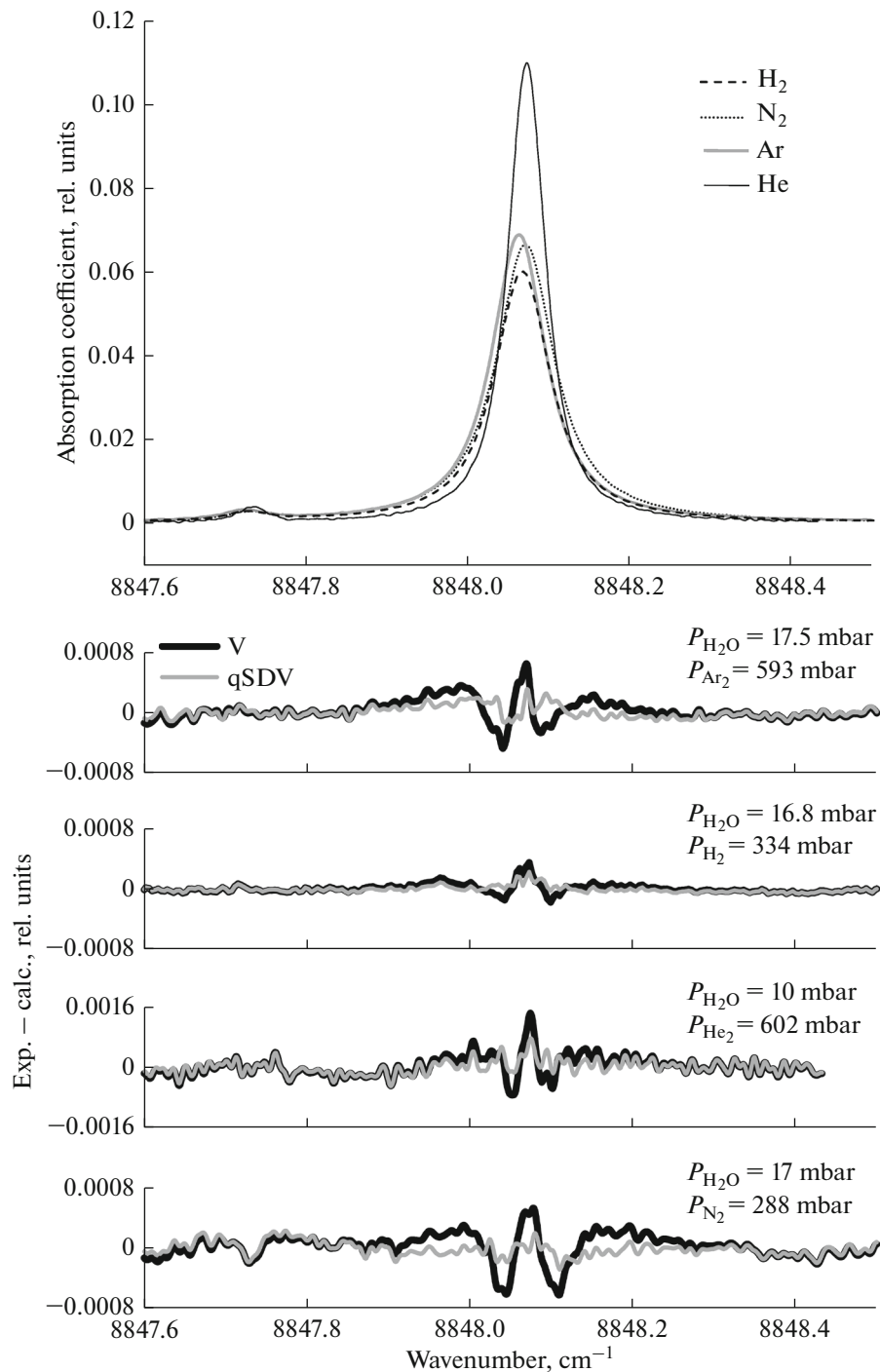
Fig. 1. H$_2$O absorption line centered at 8848.06925 cm^{-1} and broadened by H$_2$, N$_2$, Ar, and He pressure: the approximation with V and qSDV profiles.

The analysis performed shows that the traditional Voigt profile can be used for the approximation of spectral lines in the spectral region 8650–9020 cm^{-1} in problems where high accuracy of parameters is not required (for example, when determining the water vapor content in the atmosphere of planets etc.). This primarily relates to light broadening molecules, such as helium and hydrogen. If high accuracy is required, then profile models are needed, which, on the one hand, take into account fine effects, and on the other hand, are simple enough for large-scale studies with a small number of physically clear approximation parameters. The speed-dependent Voigt profile satisfies these conditions the best for buffer gas pressures of

Table 2. Coefficients of H_2O absorption lines broadening and shift by helium and argon pressure obtained with the use of the speed-dependent Voigt profile, $cm^{-1}\ atm^{-1}$

$\nu,\ cm^{-1}$ HITRAN	$J'\ K'_a\ K'_c$ $J''\ K''_a\ K''_c$	γ_{He}	δ_{He}	β_{He}	γ_{Ar}	δ_{Ar}	β_{Ar}
8830.23079	1 0 1 0 0 0	0.0235(1)	0.0012(1)	0.0032(3)	0.0478(2)	−0.0185(1)	0.0045(3)
8869.87204	3 0 3 2 0 2	0.0206(2)	0.0015(1)	0.0018(2)	0.0428(3)	−0.0208(1)	0.0061(3)
8899.69188	5 0 5 4 0 4	0.0190(1)	0.0024(1)	0.0008(1)	0.0380(2)	−0.0237(2)	0.0061(2)
8937.23296	8 0 8 7 0 7	0.0156(2)	0.0041(1)	0.0021(2)	0.0263(3)	−0.0266(2)	0.0079(3)
8948.14907	9 0 9 8 0 8	0.0159(2)	0.0046(1)	0.0026(3)	0.0238(3)	−0.0273(2)	0.0073(3)
8958.63401	10 0 10 9 0 9	0.0144(1)	0.0043(1)	0.0032(3)	0.0224(2)	−0.0257(2)	0.0071(3)
8760.13999	1 0 1 2 0 2	0.0213(1)	0.0000(1)	0.0019(2)	0.0490(3)	−0.0236(2)	0.0055(3)
8696.98670	4 0 4 5 0 5	0.0189(1)	0.0007(1)	0.0006(1)	0.0389(2)	−0.0260(1)	0.0036(2)
8652.08684	6 0 6 7 0 7	0.0171(2)	0.0020(1)	0.0017(2)	0.0320(3)	−0.0282(1)	0.0073(1)
8628.14132	7 0 7 8 0 8	0.0178(2)	0.0025(1)	0.0029(3)	0.0288(2)	−0.0282(2)	0.0087(2)
8848.06925	2 1 2 1 1 1	0.0230(1)	0.0025(1)	0.0026(3)	0.0462(2)	−0.0169(1)	0.0068(3)
8882.87188	4 1 4 3 1 3	0.0199(2)	0.0024(1)	0.0014(1)	0.0407(2)	−0.0220(2)	0.0063(1)
8912.25551	6 1 6 5 1 5	0.0187(1)	0.0028(1)	0.0030(3)	0.0342(1)	−0.0249(1)	0.0085(3)
8925.22161	7 1 7 6 1 6	0.0166(2)	0.0034(1)	0.0014(1)	0.0279(1)	−0.0255(2)	0.0060(2)
8937.13002	8 1 8 7 1 7	0.0161(1)	0.0042(1)	0.0018(2)	0.0273(2)	−0.0265(1)	0.0080(2)
8948.44132	9 1 9 8 1 8	0.0158(2)	0.0045(1)	0.0034(3)	0.0238(2)	−0.0272(2)	0.0080(3)
8957.60052	10 1 10 9 1 9	0.0142(1)	0.0048(1)	0.0031(3)	0.0212(1)	−0.0276(1)	0.0071(5)
8765.03919	1 1 1 2 1 2	0.0205(1)	0.0002(1)	0.0007(1)	0.0471(2)	−0.0254(1)	0.0030(3)
8742.92788	2 1 2 3 1 3	0.0212(1)	0.0003(1)	0.0022(2)	0.0464(3)	−0.0229(2)	0.0054(2)
8698.52490	4 1 4 5 1 5	0.0200(2)	0.0008(1)	0.0023(2)	0.0404(4)	−0.0263(1)	0.0064(2)
8675.77892	5 1 5 6 1 6	0.0179(2)	0.0013(1)	0.0019(2)	0.0358(1)	−0.0276(2)	0.0079(2)
8652.40180	6 1 6 7 1 7	0.0178(1)	0.0021(1)	0.0006(1)	0.0318(2)	−0.0279(1)	0.0070(2)
8628.31130	7 1 7 8 1 8	0.0170(1)	0.0029(1)	0.0031(3)	0.0283(3)	−0.0280(2)	0.0079(3)
8861.12402	2 1 1 1 1 0	0.0213(2)	0.0019(1)	0.0022(2)	0.0446(1)	−0.0205(1)	0.0064(3)
8955.05380	7 1 6 6 1 5	0.0205(2)	0.0036(1)	0.0039(4)	0.0355(2)	−0.0250(2)	0.0049(5)
8967.23161	8 1 7 7 1 6	0.0177(2)	0.0036(1)	0.0023(2)	0.0298(3)	−0.0259(1)	0.0027(4)
8989.79912	10 1 9 9 1 8	0.0184(2)	0.0054(1)	0.0067(7)	0.0240(2)	−0.0272(2)	0.0081(5)
8754.93163	1 1 0 2 1 1	0.0225(2)	0.0003(1)	0.0028(3)	0.0472(2)	−0.0236(2)	0.0064(4)
8730.12995	2 1 1 3 1 2	0.0206(2)	0.0017(1)	0.0018(2)	0.0407(2)	−0.0205(2)	0.0069(4)
8680.25840	4 1 3 5 1 4	0.0200(2)	0.0008(1)	0.0025(3)	0.0439(1)	−0.0246(2)	0.0082(4)
8658.07834	5 1 4 6 1 5	0.0212(2)	0.0012(1)	0.0025(3)	0.0412(2)	−0.0244(1)	0.0063(3)
8636.75707	6 1 5 7 1 6	0.0212(2)	0.0017(1)	0.0053(5)	0.0387(3)	−0.0254(2)	0.0087(5)

Table 3. Coefficients of H$_2$O absorption lines broadening and shift by hydrogen and nitrogen obtained using the speed-dependent Voigt profile, cm^{-1} atm^{-1}

| ν, cm^{-1} HITRAN	$J'\ K'_a\ K'_c$ $J''\ K''_a\ K''_c$	γ_{H_2}	δ_{H_2}	β_{H_2}	γ_{N_2}	δ_{N_2}	β_{N_2}
8830.23079	1 0 1 0 0 0	0.0898(3)	−0.0107(1)	0.0044(1)	0.1162(3)	−0.0079(1)	0.0207(3)
8869.87204	3 0 3 2 0 2	0.0801(5)	−0.0088(1)	0.0053(1)	0.1108(4)	−0.0009(1)	0.0186(3)
8899.69188	5 0 5 4 0 4	0.0605(5)	−0.0114(1)	0.0041(1)	0.0959(4)	−0.0050(1)	0.0126(4)
8937.23296	8 0 8 7 0 7	0.0434(5)	−0.0150(2)	0.0047(2)	0.0584(4)	−0.0139(1)	0.0105(5)
8948.14907	9 0 9 8 0 8	0.0403(5)	−0.0150(2)	0.0033(2)	0.0466(4)	−0.0171(2)	0.0089(4)
8958.63401	10 0 10 9 0 9	0.0461(3)	−0.0135(2)	0.0033(1)	0.0442(3)	−0.0153(1)	0.0025(3)
8760.13999	1 0 1 2 0 2	0.0857(5)	−0.0162(1)	0.0064(2)	0.1145(4)	−0.0097(1)	0.0176(4)
8696.98670	4 0 4 5 0 5	0.0594(5)	−0.0172(1)	0.0033(1)	0.0998(4)	−0.0117(1)	0.0151(5)
8652.08684	6 0 6 7 0 7	0.0473(4)	−0.0170(2)	0.0044(1)	0.0733(3)	−0.0178(2)	0.0080(3)
8628.14132	7 0 7 8 0 8	0.0443(3)	−0.0155(1)	0.0050(1)	0.0613(3)	−0.0205(1)	0.0110(4)
8848.06925	2 1 2 1 1 1	0.0914(4)	−0.0104(1)	0.0051(2)	0.1119(4)	−0.0051(1)	0.0180(3)
8882.87188	4 1 4 3 1 3	0.0679(4)	−0.0102(1)	0.0040(1)	0.0994(4)	−0.0054(1)	0.0115(2)
8912.25551	6 1 6 5 1 5	0.0510(4)	−0.0126(1)	0.0039(2)	0.0833(4)	−0.0092(1)	0.0130(3)
8925.22161	7 1 7 6 1 6	0.0495(4)	−0.0147(2)	0.0072(2)	0.0720(3)	−0.0118(1)	0.0112(4)
8937.13002	8 1 8 7 1 7	0.0429(4)	−0.0154(2)	0.0037(1)	0.0545(3)	−0.0148(1)	0.0034(3)
8948.44132	9 1 9 8 1 8	0.0411(4)	−0.0151(1)	0.0043(2)	0.0477(3)	−0.0176(2)	0.0082(2)
8957.60052	10 1 10 9 1 9	0.0436(1)	−0.0160(2)	0.0109(2)	0.0378(1)	−0.0209(2)	0.0082(2)
8765.03919	1 1 1 2 1 2	0.0925(6)	−0.0134(2)	0.0064(2)	0.1098(6)	−0.0051(2)	0.0108(2)
8742.92788	2 1 2 3 1 3	0.0805(4)	−0.0167(2)	0.0051(1)	0.1060(3)	−0.0080(2)	0.0133(1)
8698.52490	4 1 4 5 1 5	0.0594(4)	−0.0176(2)	0.0039(1)	0.0957(4)	−0.0123(2)	0.0134(4)
8675.77892	5 1 5 6 1 6	0.0521(5)	−0.0177(1)	0.0048(2)	0.0867(5)	−0.0142(1)	0.0149(4)
8652.40180	6 1 6 7 1 7	0.0469(3)	−0.0168(2)	0.0031(1)	0.0774(3)	−0.0148(1)	0.0190(3)
8628.31130	7 1 7 8 1 8	0.0441(3)	−0.0158(2)	0.0047(2)	0.0606(2)	−0.0187(1)	0.0096(4)
8861.12402	2 1 1 1 1 0	0.0887(4)	−0.0085(1)	0.0062(2)	0.1157(5)	−0.0070(1)	0.0240(3)
8955.05380	7 1 6 6 1 5	0.0597(5)	−0.0131(2)	0.0048(1)	0.0893(3)	−0.0055(2)	0.0067(2)
8967.23161	8 1 7 7 1 6	0.0526(4)	−0.0146(1)	0.0039(1)	0.0765(2)	−0.0100(2)	0.0093(3)
8989.79912	10 1 9 9 1 8	0.0460(4)	−0.0148(1)	0.0042(1)	0.0490(1)	−0.0162(1)	0.0090(3)
8754.93163	1 1 0 2 1 1	0.0891(4)	−0.0137(2)	0.0038(1)	0.0994(4)	−0.0031(1)	0.0142(4)
8730.12995	2 1 1 3 1 2	0.0867(4)	−0.0124(1)	0.0064(2)	0.1103(4)	−0.0013(1)	0.0226(5)
8680.25840	4 1 3 5 1 4	0.0743(5)	−0.0135(2)	0.0051(2)	0.1038(5)	−0.0079(1)	0.0212(5)
8658.07834	5 1 4 6 1 5	0.0673(4)	−0.0148(2)	0.0042(1)	0.0969(5)	−0.0104(2)	0.0124(4)
8636.75707	6 1 5 7 1 6	0.0607(4)	−0.0156(1)	0.0062(2)	0.0921(4)	−0.0142(2)	0.0183(4)
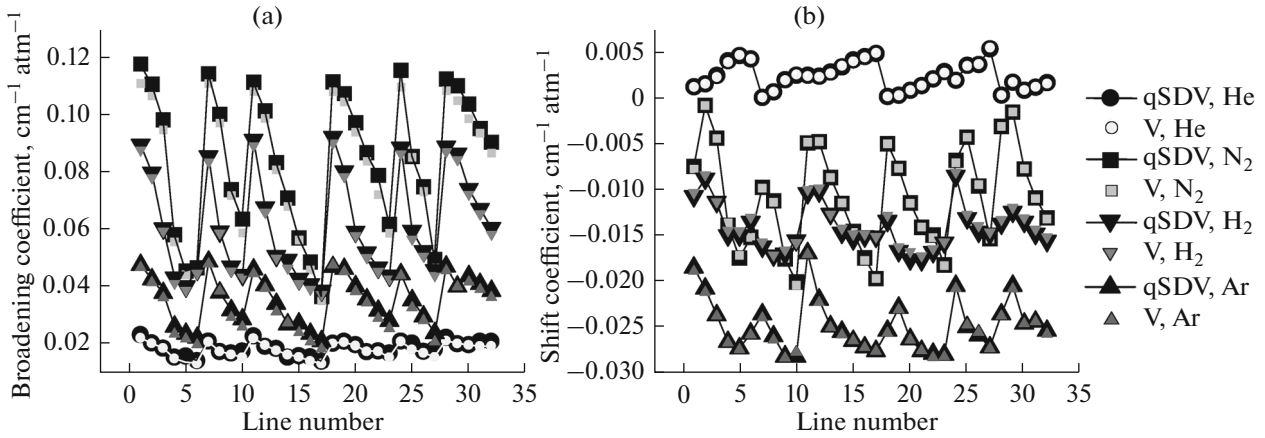
Fig. 2. Comparison between the buffer-gas (a) broadening and (b) shift coefficients of H_2O absorption lines obtained when approximating to qSDV- and V profiles (the line number corresponds to the line number in Table 2).
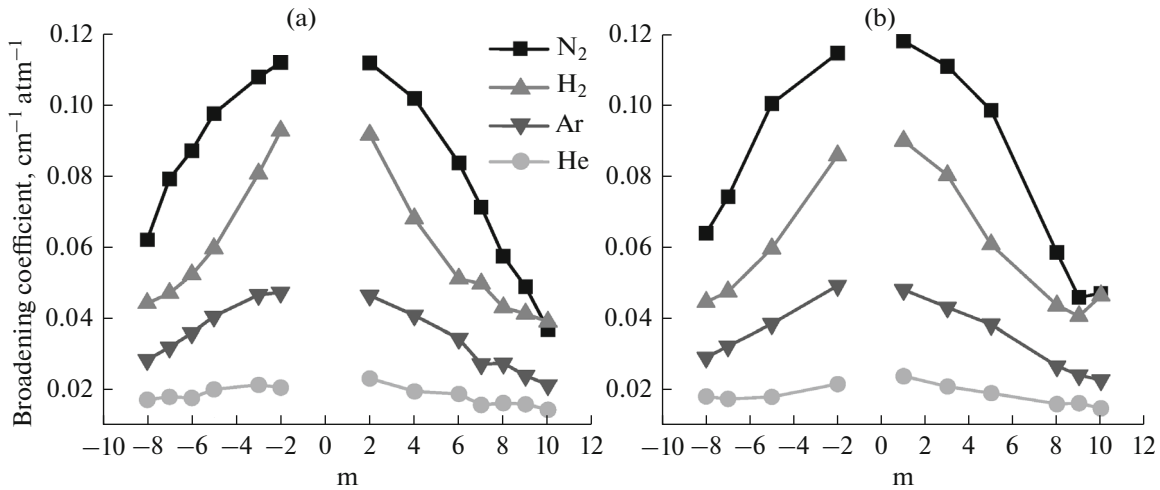

Fig. 3. Coefficient of buffer-gas (N_2, H_2, Ar, and He) broadening of H_2O molecule absorption lines as a function of the rotational quantum number m for subbranches (a) $(J\,0\,J) \leftrightarrow (J \pm 1\,0\,J \pm 1)$ and (b) $(J\,1\,J \pm 1) \leftrightarrow (J \pm 1\,1\,J \pm 1)$ (m = J'' + 1 for R- and $-J''$ for P-branch).
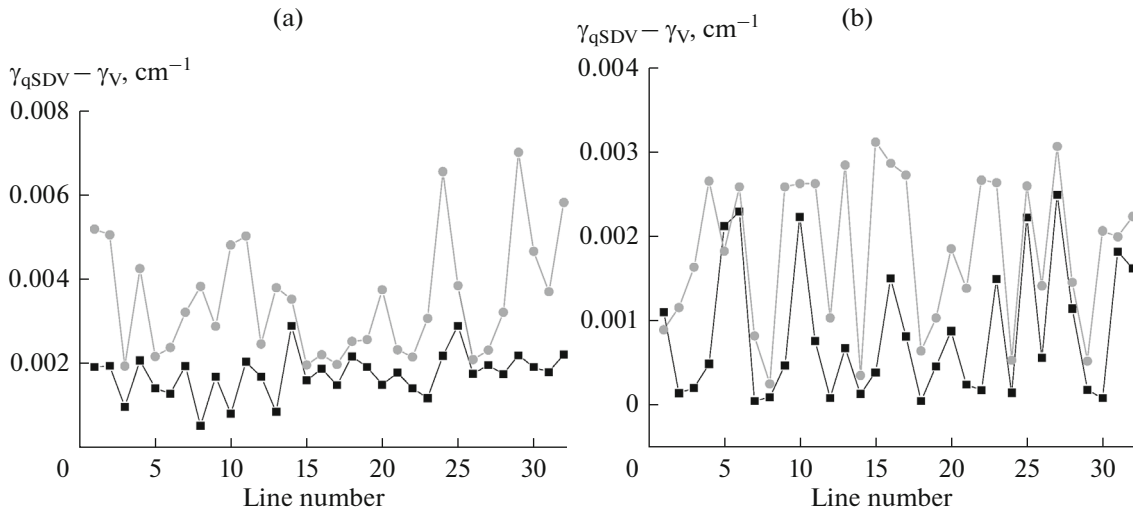

Fig. 4. Comparison between the broadening coefficients of H_2O molecule absorption lines for (a) H_2O-He (—■—) and H_2O-Ar (—●—); (b) H_2O-H_2 (—■—) and H_2O-N_2 (—●—) mixtures.

higher than 300 mbar. These results were obtained for lines with the half-widths comparable to the Doppler half-width and wider. For narrower lines, additional research is required.

FUNDING

CONFLICT OF INTEREST

The authors declare that they have no conflicts of interest.

REFERENCES

1. J.-M. Hartmann, C. Boulet, and D. Robert, *Collisional Effects on Molecular Spectra: Laboratory Experiments and Models, Consequences for Application* (Elsevier Science, Amsterdam, Boston, 2008).

2. D. Lisak, A. Cygan, D. Bermejo, J. L. Domenech, J. T. Hodges, and H. Tran, "Application of the Hartmann–Tran profile to analysis of H₂O spectra," J. Quant. Spectrosc. Radiat. Transfer **164**, 221–233 (2015).

3. N. H. Ngo, D. Lisak, H. Tran, and J.-M. Hartmann, "An isolated line-shape model to go beyond the Voigt profile in spectroscopic databases and radiative transfer codes," J. Quant. Spectrosc. Radiat. Transfer **129**, 89–100 (2013).

4. J. Tennyson, P. F. Bernath, A. Campargue, A. G. Csaszar, L. Daumont, R. R. Gamache, J. T. Hodges, D. Lisak, O. V. Naumenko, L. S. Rothman, H. Tran, N. F. Zobov, J. Buldyreva, C. D. Boone, M. D. De Vizia, L. Gianfrani, J.-M. Hartmann, R. McPheat, D. Weidmann, J. Murray, N. H. Ngo, and O. N. Polyansky, "Recommended isolated-line profile for representing high-resolution spectroscopic transitions (IUPAC Technical Report)," Pure Appl. Chem. **86** (12), 1931–1943 (2014).

5. T. M. Petrova, A. M. Solodov, A. A. Solodov, V. M. Deichuli, and V. I. Starikov, "Measurements and calculations of Ar-broadening parameters of water vapour transitions in a wide spectral region," Mol. Phys. **115** (14), 1642–1656 (2017).

6. N. N. Lavrentieva, T. M. Petrova, A. M. Solodov, and A. A. Solodov, "Measurements of N₂-broadening and shifting parameters of the water vapor spectral lines in the second hexad region," J. Quant. Spectrosc. Radiat. Transfer **111** (15), 2291–2297 (2010).

7. T. M. Petrova, A. M. Solodov, V. I. Starikov, and A. A. Solodov, "Measurements and calculations of He-broadening and -shifting parameters of the water vapor transitions of the $\nu_1 + \nu_2 + \nu_3$ band," Mol. Phys. **110** (14), 1493–1503 (2012).

8. T. M. Petrova, A. M. Solodov, A. A. Solodov, V. M. Deichuli, and V. I. Starikov, "Measurements and calculations of H₂-broadening and shift parameters of water vapour transitions of the $\nu_1 + \nu_2 + \nu_3$ band," Mol. Phys. **116** (10), 1409–1420 (2018).

9. T. M. Kruglova and A. P. Shcherbakov, "Automated line search in molecular spectra based on nonparametric statistical methods: Regularization in estimating parameters of spectral lines," Opt. Spectrosc. **111** (3), 353–356 (2011).

10. T. M. Petrova, A. M. Solodov, A. P. Shcherbakov, V. M. Deichuli, A. A. Solodov, Yu. N. Ponomarev, and T. Yu. Chesnokova, "Parameters of broadening of water molecule absorption lines by argon derived using different line profile models," Atmos. Ocean. Opt. **30** (2), 123–128 (2017).

11. C. D. Boone, "Speed-dependent Voigt profile for water vapor in infrared remote sensing applications," J. Quant. Spectrosc. Radiat. Transfer **105**, 525–532 (2007).

12. L. S. Rothman, I. E. Gordon, Y. Babikov, A. Barbe, Benner D. Chris, P. F. Bernath, M. Birk, L. Bizzocchi, V. Boudon, L. R. Brown, A. Campargue, K. Chance, E. A. Cohen, L. H. Coudert, V. M. Devi, B. J. Drouin, A. Fayt, J.-M. Flaud, R. R. Gamache, J. J. Harrison, J.-M. Hartmann, C. Hill, J. T. Hodges, D. Jacquemart, A. Jolly, J. Lamouroux, R. J. Le Roy, G. Li, D. A. Long, O. M. Lyulin, C. J. Mackie, S. T. Massie, S. Mikhailenko, H. S. P. Muller, O. V. Naumenko, A. V. Nikitin, J. Orphal, V. Perevalov, A. Perrin, E. R. Polovtseva, C. Richard, M. A. H. Smith, E. Starikova, K. Sung, S. Tashkun, J. Tennyson, G. C. Toon, Vl. G. Tyuterev, and G. Wagner, "The HITRAN2012 molecular spectroscopic database," J. Quant. Spectrosc. Radiat. Transfer **130**, 4–50 (2013).

Translated by O. Ponomareva